

Metabolites produced by commensal bacteria promote peripheral regulatory T-cell generation

Nicholas Arpaia^{1,2}, Clarissa Campbell^{1,2}, Xiying Fan^{1,2}, Stanislav Dikiy^{1,2}, Joris van der Veeken^{1,2}, Paul deRoos^{1,2}, Hui Liu³, Justin R. Cross³, Klaus Pfeffer⁴, Paul J. Coffey^{1,2,5} & Alexander Y. Rudenskiy^{1,2}

Intestinal microbes provide multicellular hosts with nutrients and confer resistance to infection. The delicate balance between pro- and anti-inflammatory mechanisms, essential for gut immune homeostasis, is affected by the composition of the commensal microbial community. Regulatory T cells (T_{reg} cells) expressing transcription factor Foxp3 have a key role in limiting inflammatory responses in the intestine¹. Although specific members of the commensal microbial community have been found to potentiate the generation of anti-inflammatory T_{reg} or pro-inflammatory T helper 17 (T_H17) cells^{2–6}, the molecular cues driving this process remain elusive. Considering the vital metabolic function afforded by commensal microorganisms, we reasoned that their metabolic by-products are sensed by cells of the immune system and affect the balance between pro- and anti-inflammatory cells. We tested this hypothesis by exploring the effect of microbial metabolites on the generation of anti-inflammatory T_{reg} cells. We found that in mice a short-chain fatty acid (SCFA), butyrate, produced by commensal microorganisms during starch fermentation, facilitated extrathymic generation of T_{reg} cells. A boost in T_{reg} -cell numbers after provision of butyrate was due to potentiation of extrathymic differentiation of T_{reg} cells, as the observed phenomenon was dependent on intronic enhancer CNS1 (conserved non-coding sequence 1), essential for extrathymic but dispensable for thymic T_{reg} -cell differentiation^{1,7}. In addition to butyrate, *de novo* T_{reg} -cell generation in the periphery was potentiated by propionate, another SCFA of microbial origin capable of histone deacetylase (HDAC) inhibition, but not acetate, which lacks this HDAC-inhibitory activity. Our results suggest that bacterial metabolites mediate communication between the commensal microbiota and the immune system, affecting the balance between pro- and anti-inflammatory mechanisms.

We explored potential mechanisms of induction of anti-inflammatory T_{reg} cells by commensal microorganisms. We considered the possibility that microbial metabolites facilitate generation of extrathymic T_{reg} cells, and if so, such products are likely to be found in the faeces of specific pathogen-free (SPF) mice with a normal spectrum of commensal microorganisms, but not in that of microbiota-deficient mice treated with broad-spectrum antibiotics (AVNM) or germ-free mice. Indeed, we found that polar solvent extracts of faeces from SPF, but not germ-free or AVNM-treated mice potentiated induction of Foxp3 after stimulation of purified peripheral naive ($CD44^{lo}CD62L^{hi}CD25^{-}$) $CD4^{+}$ T cells by CD3 antibody in the presence of dendritic cells, interleukin-2 (IL-2), and transforming growth factor- β (TGF- β) (Fig. 1a). Among bacterial metabolites we expected to find short-chain fatty acids (SCFAs), and evaluated their content in faecal extracts from SPF, germ-free or AVNM-treated mice and their ability to affect T_{reg} -cell generation. Analysis of hydrazine-derivatized SCFAs by high-performance liquid chromatography (HPLC) showed a sharp reduction in propionate and butyrate in extracts from germ-free and AVNM-treated versus SPF animals (Fig. 1b). Concentrations of these SCFAs in extracts were within a

5-mM range, corresponding to approximately 100–125 μ M *in vitro* Foxp3 induction assays (data not shown). Furthermore, purified butyrate, and to a lesser degree isovalerate and propionate, but not acetate, augmented TGF- β -dependent generation of Foxp3⁺ cells *in vitro* (Fig. 1c; data not shown). To exclude the possibility that butyrate allowed for expansion of a few contaminating T_{reg} cells in the starting naive $CD4^{+}$ T-cell population, we used mice lacking an intronic Foxp3 enhancer CNS1. These mice are selectively impaired in extrathymic T_{reg} -cell differentiation but have intact thymic differentiation^{1,7}. Butyrate failed to rescue the impaired Foxp3 induction in naive $CD4^{+}$ T cells in the absence of CNS1 (Fig. 1d). Consistent with this result, butyrate did not

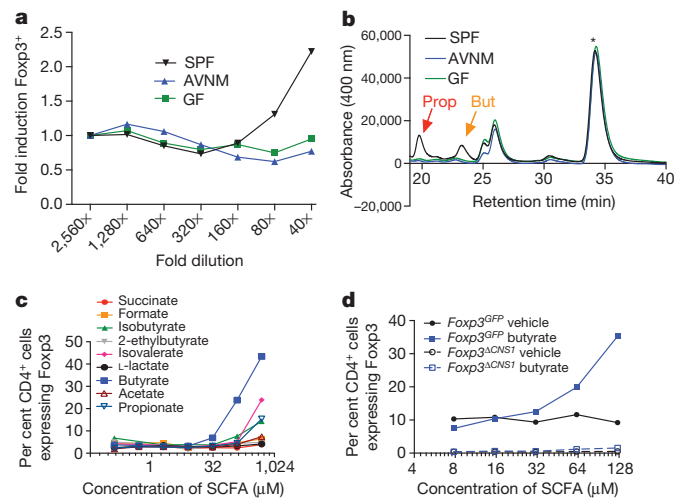


Figure 1 | SCFAs produced by commensal bacteria stimulate *in vitro* generation of T_{reg} cells. **a**, Effect of faecal extracts from specific pathogen-free (SPF), antibiotic-treated (AVNM), or germ-free (GF) mice on *in vitro* induction of Foxp3 expression in naive $CD4^{+}$ T cells stimulated with CD3 antibody in the presence of Fc γ 3-elicited dendritic cells and TGF- β . Foxp3 expression was assessed by flow cytometric analysis on day 4 of culture. Naive $CD25^{-}CD62L^{hi}CD44^{lo}CD4^{+}$ T cells were FACS-purified from B6 mice. Faecal extracts were prepared in 70% ethanol. Data are shown as fold induction over corresponding dilution of vehicle and are representative of two independent experiments. **b**, HPLC fractionation of 2-nitrophenylhydrazine-HCl-derivatized SCFAs present in indicated faecal extracts. Red and yellow arrows indicate peaks corresponding to propionate (Prop) and butyrate (But), respectively. Asterisk, internal standard peak. The HPLC fractionation profile of faecal extracts pooled from three animals each is representative of two independent experiments. **c**, Effect of indicated purified SCFAs on *in vitro* induction of Foxp3 expression in naive $CD4^{+}$ T cells isolated from B6 or Foxp3^{GFP} mice as described in **a**. Data are representative of three independent experiments. **d**, Effect of butyrate on Foxp3 induction in CNS1-sufficient and -deficient naive $CD4^{+}$ T cells from Foxp3^{GFP} and Foxp3^{CNS1} mice as described in **a**. Data are representative of two or more independent experiments.

¹Howard Hughes Medical Institute and Ludwig Center at Memorial Sloan-Kettering Cancer Center, New York, New York 10065, USA. ²Immunology Program, Memorial Sloan-Kettering Cancer Center, New York, New York 10065, USA. ³Donald B. and Catherine C. Marron Cancer Metabolism Center, Memorial Sloan-Kettering Cancer Center, New York, New York 10065, USA. ⁴Institute of Medical Microbiology and Hospital Hygiene, Heinrich-Heine-University Duesseldorf, Duesseldorf 40225, Germany. ⁵Department of Cell Biology, University Medical Center Utrecht, 3584 CX Utrecht, The Netherlands.

diminish either qualitatively or quantitatively the TGF- β dependence of Foxp3 induction in CNS1-sufficient CD4⁺ T cells (data not shown). These data suggest that butyrate promotes extrathymic differentiation of T_{reg} cells.

To determine whether butyrate is capable of promoting extrathymic T_{reg}-cell generation *in vivo*, we administered butyrate in drinking water to AVNM-treated mice, which exhibit a sharp decrease in microbially derived SCFAs, or untreated control SPF mice. Although we detected only very modest changes, if any, in the lymph node and splenic T_{reg}-cell subsets in control mice, provision of butyrate to AVNM-treated animals resulted in a robust increase in peripheral, but not thymic or colonic T_{reg} cells (Fig. 2a, b and Supplementary Fig. 1; data not shown). This increase was not an indirect consequence of an inflammatory response because non-lymphoid tissue histology and production of T_{H1}, T_{H2}, and T_{H17} cytokines by Foxp3⁻ CD4⁺ T cells remained unchanged after butyrate treatment (data not shown; Supplementary Fig. 2). In agreement with the observed CNS1 dependence of *in vitro* Foxp3 induction, provision of butyrate to AVNM-treated CNS1-deficient mice did not increase the proportion or absolute numbers of T_{reg} cells (Fig. 2c; data not shown). Thus, the observed butyrate-mediated increase in the T_{reg} cell subset *in vivo* was due to

increased extrathymic generation of T_{reg} cells and not due to their increased thymic output¹⁷. To ensure that butyrate reconstitution did not result in its non-physiologically high levels, we used liquid chromatography–mass spectrometry (LC–MS) to compare amounts of butyrate in the serum of AVNM-treated mice that received butyrate versus amounts found in control SPF mice. Although virtually undetectable in AVNM-treated CNS1-sufficient and -deficient animals, butyrate provision resulted in serum levels comparable to those found in unperturbed SPF mice that did not receive butyrate (Fig. 2d). Consistent with the aforementioned unchanged colonic T_{reg}-cell subset in AVNM-treated mice that received butyrate in their drinking water, levels of butyrate in faecal pellets were not reconstituted in these mice, possibly owing to its uptake in the small intestine or stomach (data not shown). In contrast, delivery of butyrate by enema into the colon of CNS1-sufficient, but not CNS1-deficient mice, led to an increase in the T_{reg}-cell subset in the colonic lamina propria (Fig. 2e). Thus, local provision of butyrate promoted CNS1-dependent extrathymic generation of T_{reg} cells in the colon. Furthermore, feeding mice butyrylated starch, in the absence of antibiotic treatment, increased colonic T_{reg}-cell subsets in comparison to a control starch diet (Supplementary Fig. 3)⁸. In addition to increasing T_{reg}-cell numbers, restoration of butyrate levels in AVNM-treated animals did not decrease, but instead increased intracellular Foxp3 protein amounts on a per-cell basis in both CNS1-sufficient and -deficient mice, suggesting that this bacterial metabolite may also buttress pre-existing T_{reg}-cell populations through stabilization of Foxp3 protein expression (Fig. 2f; data not shown).

In contrast to butyrate's ability to increase T_{reg}-cell generation in the colon only after local, but not systemic delivery, other SCFAs, namely acetate and propionate, were recently shown to promote accumulation of T_{reg} cells in the colon by activating GPR43 (ref. 9). These results suggest discrete modes of action of these three SCFAs. To test this idea we administered AVNM-treated CNS1-sufficient and -deficient mice with propionate and acetate in drinking water. Similarly to butyrate, oral provision of propionate increased T_{reg}-cell subsets in the spleen in AVNM-treated CNS1-sufficient, but not -deficient animals, suggesting that propionate also promotes *de novo* generation of peripheral

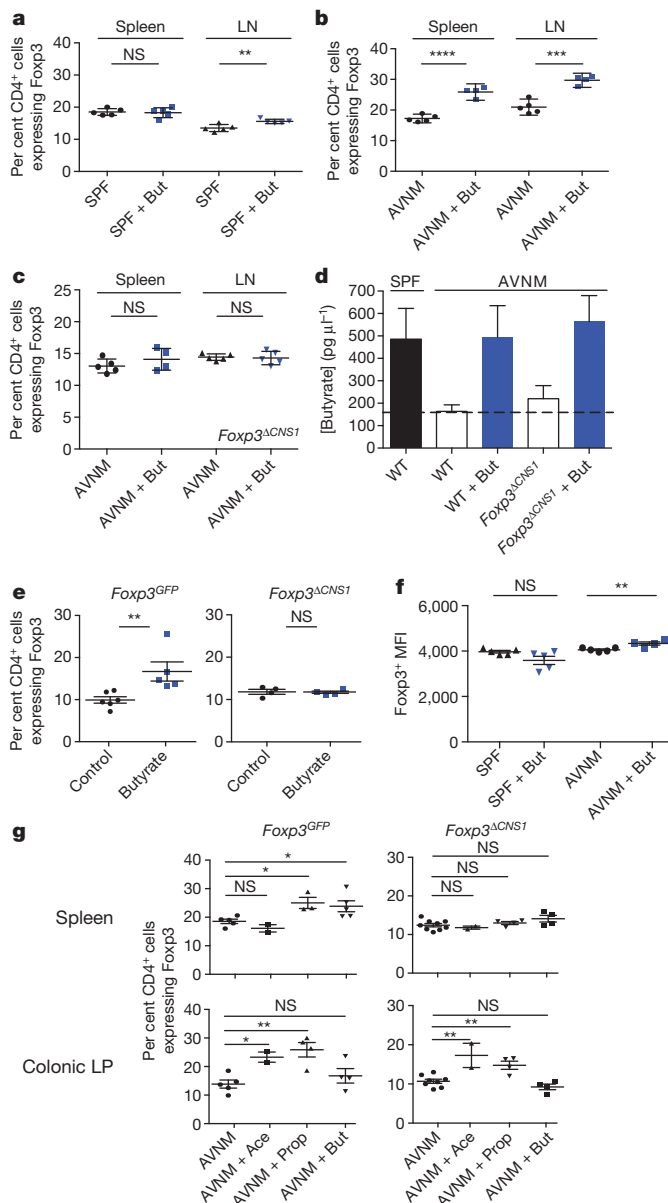


Figure 2 | Butyrate provision promotes extrathymic T_{reg}-cell generation *in vivo*. **a, b**, Flow cytometric analysis of Foxp3⁺ T_{reg}-cell subsets in the spleen and lymph nodes (LNs) of AVNM-treated (AVNM) or untreated (specific pathogen-free; SPF) B6 or *Foxp3^{GFP}* mice treated with (+But; blue symbols) or without (black symbols) butyrate in drinking water. Data are representative of three independent experiments. **c**, CNS1-deficient mice were treated with AVNM with or without butyrate as in **a** and analysed for Foxp3 expression in splenic and lymph node CD4⁺ T-cell populations. Data are representative of two independent experiments. **d**, LC–MS analysis of butyrate in serum from CNS1-sufficient B6 (wild-type; WT) and -deficient mice (*Foxp3^{ΔCNS1}*) treated as in **a**. Serum was derivatized with 2-nitrophenylhydrazine-HCl. Butyrate levels in serum of untreated (SPF) B6 mice are shown in black. AVNM WT and CNS1-deficient animals supplemented with (+But; solid bars) or without (empty bars) butyrate are shown. At least four mice per group; error bars, s.e.m. **e**, Flow cytometric analysis of Foxp3⁺ T_{reg}-cell populations in colonic lamina propria of *Foxp3^{GFP}* (left) and CNS1-deficient mice (right). Mice were administered butyrate (blue symbols) or pH-matched water (control; black symbols) by enema for 7 days and analysed for Foxp3 expression in colonic CD4⁺ T-cell populations. The data represent the combination of two independent experiments; error bars, s.e.m. **f**, Flow cytometric analysis of Foxp3 protein expression on a per-cell basis in splenic Foxp3⁺ T_{reg} cells in B6 mice treated with butyrate (+But) alone (SPF) or in combination with antibiotics (AVNM) as indicated. The data are shown as mean fluorescence intensity (MFI) ± s.d. Data are representative of at least three independent experiments. **g**, AVNM-treated *Foxp3^{GFP}* (left) and CNS1-deficient (right) mice were administered acetate (Ace), propionate (Prop), butyrate (But) or no SCFA (AVNM) for a period of 3 weeks. This was followed by analysis of Foxp3⁺ T_{reg}-cell subsets within CD4⁺ cells isolated from the colonic lamina propria (top panels) or spleens (bottom panels). Data represent the combination of two independent experiments; error bars, s.e.m. **P* ≤ 0.05, ***P* ≤ 0.01, ****P* ≤ 0.001.

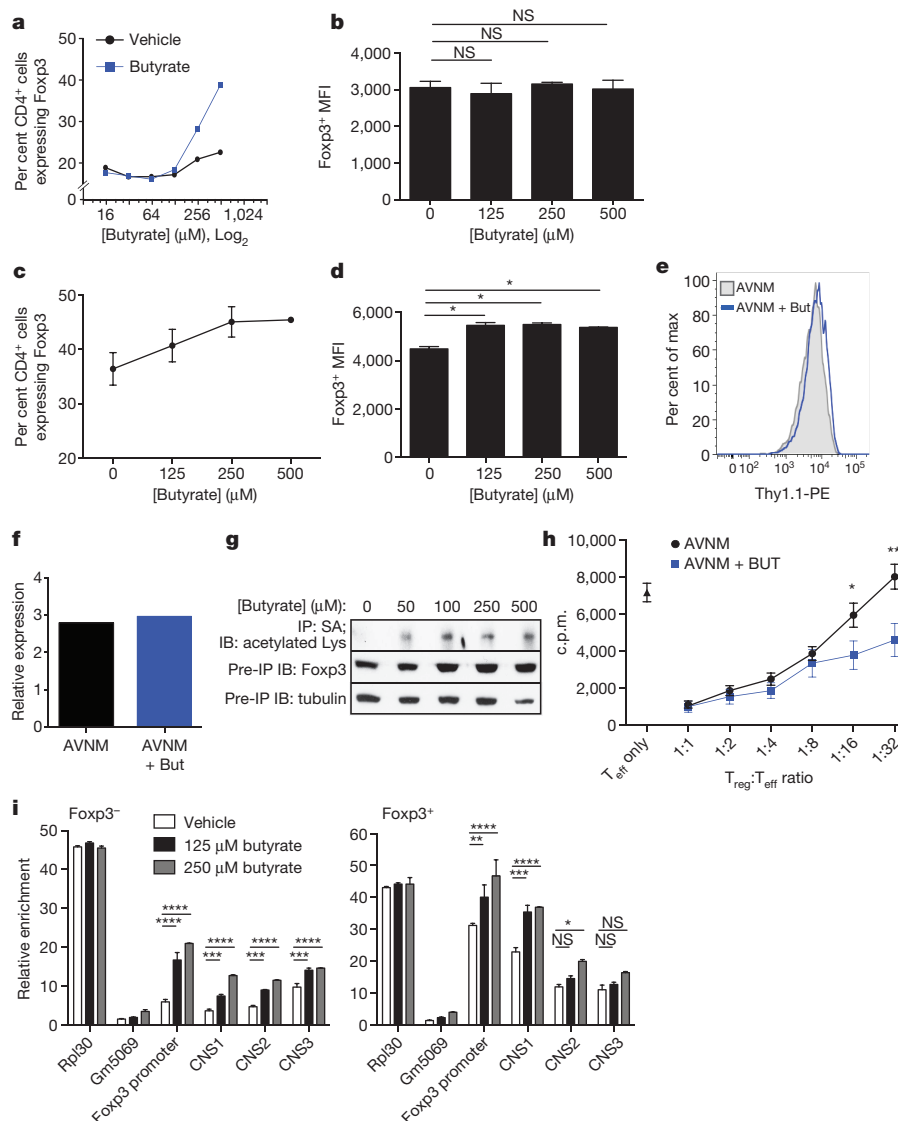


Figure 3 | Butyrate acts within T cells to enhance acetylation of the *Foxp3* locus and *Foxp3* protein.

a, Induction of *Foxp3* expression after stimulation of naive $CD4^+$ T cells by CD3 antibody in the presence of butyrate-treated or untreated Flt3l-elicited dendritic cells (DCs) and TGF- β . DCs were cultured with titrated amounts of butyrate or medium alone for 6 h, washed and co-cultured with FACS-purified naive $CD4^+$ T cells in the presence of CD3 antibody and TGF- β . The data are shown as per cent $CD4^+$ cells expressing *Foxp3* after 4 days of culture. Data are representative of at least four independent experiments. **b**, Analysis of *Foxp3* protein expression on a per-cell basis in T_{reg} cells generated in the presence of butyrate pre-treated Flt3l-elicited dendritic cells (as in **a**). The data are shown as mean fluorescence intensity (MFI); error bars, s.e.m. **c**, Per cent of $CD4^+$ cells expressing *Foxp3* after 4 days in FACS-sorted naive $CD4^+$ T cells incubated with CD3 and CD28 antibody-coated beads under T_{reg} -inducing conditions. Data are representative of two or more independent experiments; error bars, s.e.m. **d**, MFI of *Foxp3* expression in $Foxp3^+$ $CD4^+$ cells from **c**. Data are representative of two or more independent experiments; error bars, s.e.m. **e**, *Thy1.1* expression in $CD4^+$ $Foxp3^+$ splenocytes isolated from bi-cistronic *Foxp3^{Thy1.1}* reporter mice treated with AVNM with (+But) or without butyrate as described in Fig. 2a. Cell-surface expression of internal ribosome entry site (IRES)-driven *Thy1.1* reporter inserted into the endogenous *Foxp3* locus reflects *Foxp3* mRNA levels. The data are representative of at least three mice in each group and of two independent experiments. PE, phycoerythrin. **f**, $CD4^+$ $Foxp3^+$ splenocytes from *Foxp3^{GFP}*

reporter mice treated with AVNM with or without butyrate (as in Fig. 2a) were FACS-sorted and analysed for *Foxp3* mRNA expression by qPCR. **g**, AVI (endogenously biotinylated peptide-tagged) *Foxp3*-expressing TCLI hybridoma cells were treated for 15 h with butyrate at the indicated concentrations followed by immunoprecipitation (IP) of tagged *Foxp3* protein using streptavidin (SA) beads and immunoblot (IB) analysis for acetylated-lysine residues (top panel), total *Foxp3* protein (middle panel) and tubulin (bottom panel) from pre-precipitation whole-cell lysate. Data are representative of two independent experiments. **h**, Analysis of suppressor capacity of GFP^+ T_{reg} cells sorted from antibiotic-treated (AVNM) *Foxp3^{GFP}* mice administered (+But) or not administered butyrate in drinking water. Data represent two independent experiments combined, with four or more mice per group each. T_{eff} T effector cells, FACS-sorted $CD4^+$ $Foxp3^-$ naive T cells; error bars, s.e.m. **i**, FACS-sorted naive $CD4^+$ T cells isolated from *Foxp3^{GFP}* animals were incubated with CD3 and CD28 antibody-coated beads under T_{reg} -inducing conditions in the presence of indicated amounts of butyrate. $Foxp3^+$ and $Foxp3^-$ $CD4^+$ cells were FACS-purified at day 3 of culture and H3K27 acetylation at the *Foxp3* promoter and CNS1, CNS2 and CNS3 enhancers was assessed using ChIP-qPCR. Enrichment over input for each indicated *Foxp3* regulatory region at given concentrations of butyrate is shown. Data in this figure are representative of two or more independent experiments. The data represent mean \pm s.e.m. * $P \leq 0.05$, ** $P \leq 0.01$, *** $P \leq 0.001$, **** $P \leq 0.0001$, as determined by Student's *t*-test. NS, not significant.

T_{reg} cells (Fig. 2g). In contrast, acetate did not increase splenic T_{reg} -cell numbers. These results were fully consistent with our *in vitro* T_{reg} -cell differentiation studies (Fig. 1c). However, in the colon, both acetate

and propionate, but not butyrate, promoted accumulation of T_{reg} cells in a CNS1-independent manner (Fig. 2g). These results suggest that butyrate promotes *de novo* generation but not colonic accumulation of

T_{reg} cells, whereas acetate has a diametrically opposite activity and propionate is capable of both.

The observation that butyrate facilitates extrathymic differentiation of T_{reg} cells raised a question as to whether butyrate directly affects T cells or dendritic cells (or both) by enhancing their ability to induce Foxp3 expression. To explore these non-mutually exclusive possibilities, we assessed the effects of butyrate on the ability of T cells and dendritic cells to generate T_{reg} cells *in vitro* (Fig. 3a–d). We found that butyrate increased, albeit modestly (<1.5-fold), the numbers of Foxp3⁺ cells in dendritic cell-free cultures of purified naive CD4⁺ T cells stimulated by CD3 and CD28 antibody-coated beads and TGF- β (Fig. 3c). Similar to T_{reg} cells isolated from butyrate-treated mice, T_{reg} cells generated in the presence of butyrate *in vitro* expressed not lower, but rather higher amounts of Foxp3 protein on a per-cell basis than those from butyrate-free cultures (Fig. 3d). This effect was not associated with increased Foxp3 messenger RNA levels (Fig. 3e, f). Instead, it is likely to be due to increased Foxp3 protein acetylation observed in the presence of butyrate, a known histone deacetylase (HDAC) inhibitor (Fig. 3g). Foxp3 acetylation confers greater stability and enhanced function^{10–13}. Furthermore, the suppressor activity of T_{reg} cells isolated from mice treated with AVNM and butyrate was not attenuated, but was moderately enhanced compared to mice treated with AVNM alone (Fig. 3h).

Previous *in vitro* studies suggested that a synthetic HDAC inhibitor, trichostatin A (TSA), potentiates T_{reg}-cell generation *in vitro* by acting on T cells^{14,15}. As butyrate can also boost extrathymic T_{reg}-cell generation by acting directly on T cells in the absence of dendritic cells (Fig. 3c), we assessed the effect of butyrate on histone modification at the *Foxp3* locus. When naive CD4⁺ T cells from *Foxp3*^{GFP} mice, which express a green fluorescent protein (GFP) reporter fused to Foxp3, were stimulated by CD3 and CD28 antibody-coated beads and TGF- β with or without butyrate for 3 days, a marked threefold increase in acetylated histone H3 at lysine 27 (acetylated H3K27) at the *Foxp3* promoter and CNS1 enhancer was observed in Foxp3⁺ cells purified from these cultures (Fig. 3i). In contrast, increases in the acetylated H3K27 occupancy in their Foxp3⁺ counterparts were expectedly minor (~30%) and inconsequential. Accordingly, *Foxp3* mRNA levels were not different in Foxp3⁺ cells in the presence or absence of butyrate (Fig. 3e, f). Although we cannot discriminate between the contribution of increased acetylation of histone versus non-histone targets to heightened Foxp3 induction, it is likely to be facilitated by the increase in acetylated H3K27 observed in Foxp3⁺ T cells.

In addition to its direct T_{reg}-cell differentiation-promoting effects on CD4⁺ T cell precursors, butyrate endowed dendritic cells with a superior ability to facilitate T_{reg}-cell differentiation. Pre-treatment of dendritic cells with butyrate *in vitro* for 6 h followed by its removal markedly enhanced their ability to induce Foxp3 expression in naive CD4⁺ T cells stimulated by CD3 antibody and TGF- β in the absence of butyrate (Fig. 3a and Supplementary Fig. 4a, b). This treatment had no detrimental effect on dendritic-cell viability (Supplementary Fig. 4c). The Foxp3 protein expression induced by butyrate-pre-treated and control dendritic cells was comparable, in contrast to a T-cell-intrinsic effect of butyrate leading to increased amounts of Foxp3 protein in T_{reg} cells in mice treated with AVNM and butyrate (Figs 2f and 3b).

We considered butyrate sensing by G-protein-coupled receptors (GPRs) as a potential mechanism for the increase in extrathymic differentiation of T_{reg} cells^{16,17}. However, pre-treatment of *Gpr109a*^{+/+} and *Gpr109a*^{-/-} dendritic cells with butyrate similarly increased *in vitro* generation of Foxp3⁺ cells (Supplementary Fig. 5a). Consistent with these results, butyrate-dependent potentiation of Foxp3 induction by dendritic cells remained unchanged after pre-treatment with pertussis toxin (Supplementary Fig. 5b)¹⁸. Next, we tested HDAC inhibitory activity of butyrate and other SCFAs in dendritic cells using histone H3 acetylation as an indirect readout (Fig. 4a). Trichostatin A (TSA) and valproate, two chemically distinct HDAC inhibitors, and phenylbutyrate, a butyrate derivative with a relatively weak inhibitory activity, were used as controls in these experiments. Relative HDAC inhibitory activity

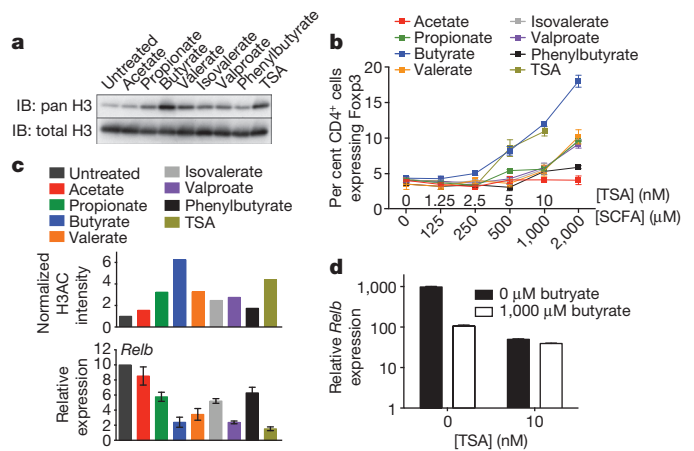


Figure 4 | HDAC-inhibitory activity of butyrate decreases pro-inflammatory cytokine expression within dendritic cells to promote T_{reg} induction. **a**, Histone acetylation in Flt3l-elicited dendritic cells from B6 mice treated with the indicated SCFA (500 μ M) or TSA (10 nM) for 6 h followed by acid extraction of histones from isolated nuclei, SDS-PAGE and blotting with antibody for pan-acetylated H3 (pan H3). Total histone H3 serving as a loading control. Shown is the relative acetylated H3 band intensity calculated over total H3 and normalized as fold over untreated. **b**, Induction of Foxp3 expression after stimulation of naive CD4⁺ T cells by CD3 antibody in the presence of SCFA or TSA, Flt3l-elicited dendritic cells and TGF- β . Dendritic cells were cultured with titrated amounts SCFA or TSA for 6 h, washed and co-cultured with FACS-purified naive CD4⁺ T cells in the presence of CD3 antibody and TGF- β . The data are shown as per cent CD4⁺ cells expressing Foxp3 after 4 days of culture. Data are representative of two or more independent experiments. **c**, *Relb* gene expression quantified by qPCR in purified Flt3l-elicited dendritic cells from B6 mice treated for 6 h with SCFA or TSA, as in **a**. Data are representative of four independent experiments. **d**, *Relb* gene expression quantified by qPCR in purified Flt3l-elicited dendritic cells from B6 mice treated with or without TSA in combination with, or in the absence of, butyrate at the indicated concentrations. Data in this figure are representative of two or more independent experiments, unless otherwise noted. The data represent mean \pm s.e.m.

of SCFAs closely correlated with their ability to potentiate the capacity of dendritic cells to induce T_{reg}-cell differentiation. Dendritic cells briefly exposed to butyrate, TSA, and to a lesser extent propionate, but not acetate, potently induced Foxp3 expression (Fig. 4b). Furthermore, microarray analysis showed that butyrate and TSA induced remarkably similar, if not identical, gene-expression changes in dendritic cells (Supplementary Fig. 6a) with a systemic repression of lipopolysaccharide (LPS) response genes including *Il-12*, *Il-6* and *Relb* (Supplementary Fig. 6b, c). Interestingly, repression of *Relb*, a major inducer of dendritic-cell activation, correlated with the level of HDAC-inhibitory activity of butyrate and other SCFAs (Fig. 4c)¹⁹. Notably, knockdown of *Relb* expression in dendritic cells promotes their ability to support T_{reg}-cell differentiation^{20,21}. To further ascertain whether TSA and butyrate potentiated T_{reg}-cell generation through HDAC inhibition and not through distinct independent mechanisms, we treated dendritic cells with the combination of butyrate and optimal amounts of TSA. If butyrate and TSA were to act through independent mechanisms, they should have exhibited synergistic effects on Foxp3 induction. However, if they acted on identical or related targets (that is, HDACs), additive effects were unlikely. We found that butyrate was unable to further enhance the ability of TSA to down-regulate *Relb* and promote Foxp3 induction (Fig. 4d; Supplementary Fig. 6d), suggesting that they act on identical or related targets. These results are consistent with the idea that the HDAC inhibitory activity of butyrate as well as propionate contributes to the ability of dendritic cells to facilitate extrathymic T_{reg}-cell differentiation.

In conclusion, our studies suggest that butyrate and propionate, produced by commensal microorganisms, increase extrathymic CNS1-dependent differentiation of T_{reg} cells. Our results indicate that metabolic

by-products of commensal microorganisms influence the balance between pro- and anti-inflammatory cells and serve as a means of communication between the commensal microbial community and the immune system.

METHODS SUMMARY

CNS1 knockout (*Foxp3^{ACNS1}*), *Foxp3^{GFP}*, *Foxp3^{Thy1.1}* and *Foxp3^{DTR}* mice have been described previously^{7,22,23}. Male C57BL/6 mice were purchased from The Jackson Laboratory. All strains were maintained in the Sloan-Kettering Institute animal facility in accordance with institutional guidelines. For antibiotic treatment, mice were given 1 g l⁻¹ metronidazole (Sigma-Aldrich), 0.5 g l⁻¹ vancomycin (Hospira), 1 g l⁻¹ ampicillin (Sigma-Aldrich) and 1 g l⁻¹ kanamycin (Fisher Scientific) in drinking water (AVNM). For butyrate, acetate and propionate administration, each SCFA was added to AVNM-containing drinking water at 36 mM and pH-adjusted as needed. Dendritic cells were expanded *in vivo* by subcutaneous injection of B16 melanoma cells secreting FLT3-ligand and purified using CD11c (N418) magnetic beads (Dynabeads, Invitrogen). *In vitro* Foxp3 induction assays were performed by incubating 5.5 × 10⁴ naive CD44^{lo}CD62L^{hi}CD25⁻CD4⁺ T cells sorted by FACS, in 1 μg ml⁻¹ of CD3 antibody in the presence of dendritic cells in 96-well flat-bottom plates for 4 days. Alternatively, naive CD4⁺ T cells were stimulated with CD3 and CD28 antibody-coated beads (Dynabeads Mouse T-Activator, Invitrogen) at a 1:1 cell-to-bead ratio. All cultures were supplemented with 1 ng ml⁻¹ TGF-β and 100 units ml⁻¹ IL-2. Intracellular staining for IL-17, interferon-γ (IFN-γ), IL-4, IL-13 and Foxp3 was performed using the Foxp3 staining kit (eBiosciences). Cytokine staining was performed after re-stimulation of *ex vivo* isolated cells with 5 μg ml⁻¹ CD3 antibody and 5 μg ml⁻¹ CD28 antibody in the presence of Golgi-plug (BD Biosciences) for 5 h. Stool samples were collected directly into sterile tubes from live mice and snap-frozen before preparation of material for SCFA quantification by HPLC or LC-MS. HPLC analysis of 2-nitrophenylhydrazine HCl-derivatized SCFAs present in stool extracts was performed as described elsewhere²⁴. Acetylated H3K27 chromatin immunoprecipitation (ChIP) quantitative polymerase chain reaction (qPCR) was performed as previously described²⁵.

Online Content Any additional Methods, Extended Data display items and Source Data are available in the online version of the paper; references unique to these sections appear only in the online paper.

Received 20 June; accepted 30 September 2013.

Published online 13 November 2013.

- Josefowicz, S. Z. *et al.* Extrathymically generated regulatory T cells control mucosal T_H2 inflammation. *Nature* **482**, 395–399 (2012).
- Round, J. L. & Mazmanian, S. K. Inducible Foxp3⁺ regulatory T-cell development by a commensal bacterium of the intestinal microbiota. *Proc. Natl Acad. Sci. USA* **107**, 12204–12209 (2010).
- Ivanov, I. I. *et al.* Induction of intestinal T_H17 cells by segmented filamentous bacteria. *Cell* **139**, 485–498 (2009).
- Lathrop, S. K. *et al.* Peripheral education of the immune system by colonic commensal microbiota. *Nature* **478**, 250–254 (2011).
- Atarashi, K. *et al.* Induction of colonic regulatory T cells by indigenous clostridium species. *Science* **331**, 337–341 (2011).
- Atarashi, K. *et al.* T_{reg} induction by a rationally selected mixture of Clostridia strains from the human microbiota. *Nature* **500**, 232–236 (2013).
- Zheng, Y. *et al.* Role of conserved non-coding DNA elements in the *Foxp3* gene in regulatory T-cell fate. *Nature* **463**, 808–812 (2010).
- Annisson, G., Illman, R. J. & Topping, D. L. Acetylated, propionylated or butyrylated starches raise large bowel short-chain fatty acids preferentially when fed to rats. *J. Nutr.* **133**, 3523–3528 (2003).
- Smith, P. M. *et al.* The microbial metabolites, short-chain fatty acids, regulate colonic T_{reg} cell homeostasis. *Science* **341**, 569–573 (2013).
- van Loosdregt, J. *et al.* Rapid temporal control of Foxp3 protein degradation by siRNA-1. *PLoS ONE* **6**, e19047 (2011).
- van Loosdregt, J. *et al.* Regulation of T_{reg} functionality by acetylation-mediated Foxp3 protein stabilization. *Blood* **115**, 965–974 (2010).
- Zhang, H., Xiao, Y., Zhu, Z., Li, B. & Greene, M. I. Immune regulation by histone deacetylases: a focus on the alteration of FOXP3 activity. *Immunol. Cell Biol.* **90**, 95–100 (2012).
- Song, X. *et al.* Structural and biological features of FOXP3 dimerization relevant to regulatory T cell function. *Cell Rep.* **1**, 665–675 (2012).
- Wang, L., de Zoeten, E. F., Greene, M. I. & Hancock, W. W. Immunomodulatory effects of deacetylase inhibitors: therapeutic targeting of FOXP3⁺ regulatory T cells. *Nature Rev. Drug Discov.* **8**, 969–981 (2009).
- Tao, R. *et al.* Deacetylase inhibition promotes the generation and function of regulatory T cells. *Nature Med.* **13**, 1299–1307 (2007).
- Maslowski, K. M. *et al.* Regulation of inflammatory responses by gut microbiota and chemoattractant receptor GPR43. *Nature* **461**, 1282–1286 (2009).
- Thangaraju, M. *et al.* GPR109A is a G-protein-coupled receptor for the bacterial fermentation product butyrate and functions as a tumor suppressor in colon. *Cancer Res.* **69**, 2826–2832 (2009).
- Nilsson, N. E., Kotarsky, K., Owman, C. & Olde, B. Identification of a free fatty acid receptor, FFA2R, expressed on leukocytes and activated by short-chain fatty acids. *Biochem. Biophys. Res. Commun.* **303**, 1047–1052 (2003).
- MacDonald, K. P. *et al.* Effector and regulatory T-cell function is differentially regulated by RelB within antigen-presenting cells during GVHD. *Blood* **109**, 5049–5057 (2007).
- Zhu, H. C. *et al.* Tolerogenic dendritic cells generated by RelB silencing using shRNA prevent acute rejection. *Cell Immunol.* **274**, 12–18 (2012).
- Shih, V. F. *et al.* Control of RelB during dendritic cell activation integrates canonical and noncanonical NF-κB pathways. *Nature Immunol.* **13**, 1162–1170 (2012).
- Fontenot, J. D. *et al.* Regulatory T cell lineage specification by the forkhead transcription factor Foxp3. *Immunity* **22**, 329–341 (2005).
- Kim, J. M., Rasmussen, J. P. & Rudensky, A. Y. Regulatory T cells prevent catastrophic autoimmunity throughout the lifespan of mice. *Nature Immunol.* **8**, 191–197 (2007).
- Torii, T. *et al.* Measurement of short-chain fatty acids in human faeces using high-performance liquid chromatography: specimen stability. *Ann. Clin. Biochem.* **47**, 447–452 (2010).
- Samstein, R. M. *et al.* Foxp3 exploits a pre-existent enhancer landscape for regulatory T cell lineage specification. *Cell* **151**, 153–166 (2012).

Supplementary Information is available in the online version of the paper.

Acknowledgements This work was supported by the Robert Black Fellowship of the Damon Runyon Cancer Research Foundation DRG-2143-13 (N.A.), Ludwig Center at Memorial Sloan Kettering Cancer Center and the US National Institutes of Health (NIH) grant T32 A1007621 (N.A.) and R37 AI034206 (A.Y.R.). A.Y.R. is an investigator with the Howard Hughes Medical Institute.

Author Contributions N.A., C.C. and X.F. performed experiments and analysed data, with general assistance from S.D. and assistance from P.d. for HPLC, P.J.C. for immunoprecipitation of acetylated Foxp3 and J.v.d.v. for ChIP-qPCR experiments. H.L. and J.R.C. performed LC-MS. N.A., C.C., X.F. and A.Y.R. designed and interpreted experiments. K.P. provided *Gpr109a* mice. N.A. and A.Y.R. wrote the paper.

Author Information Microarray data have been deposited in the Gene Expression Omnibus (GEO) under accession number GSE51263. Reprints and permissions information is available at www.nature.com/reprints. The authors declare no competing financial interests. Readers are welcome to comment on the online version of the paper. Correspondence and requests for materials should be addressed to A.Y.R. (rudenska@mskcc.org).

METHODS

Mice. *Foxp3^{ΔCNS1}* (CNS1 knockout), *Foxp3^{GFP}*, *Foxp3^{Thy1.1}* and *Gpr109a^{-/-}* mice have been previously described^{7,22,23}. Male C57BL/6 (B6) mice were purchased from the Jackson Laboratory and groups of five co-housed mice were randomly assigned to treatment versus control groups after confirmation that age and weight were in accordance between groups. Male mice were used for all experiments. All strains were maintained in the Sloan-Kettering Institute animal facility in accordance with institutional guidelines. Mice were killed by CO₂ asphyxiation then processed for tissue collection thereafter. This was carried with the experimenter blind to the group to which each mouse belonged. For antibiotic treatment, mice at 5 to 6 weeks of age were treated with 1 g l⁻¹ metronidazole (Sigma-Aldrich), 0.5 g l⁻¹ vancomycin (Hospira), 1 g l⁻¹ ampicillin (Sigma-Aldrich) and 1 g l⁻¹ kanamycin (Fisher Scientific) dissolved in drinking water. For butyrate, acetate and propionate administration, each SCFA was added to drinking water containing antibiotics (as described above) at a final concentration of 36 mM and pH-adjusted, if needed, to match that of antibiotic-only water. Butyrate was administered to mice after prior treatment with antibiotics for at least 1 week.

Cell isolation and FACS staining. For *in vitro* experiments, CD4⁺ T cells and CD11c⁺ dendritic cells were enriched using mouse CD4 (L3T4, Invitrogen) and mouse CD11c (N418, BioLegend) antibodies, respectively, that were biotinylated for use with Streptavidin Dynabeads (Invitrogen). Enriched cells were then sorted on a FACSARIA II cell sorter (BD Biosciences) for *in vitro* assays. Intracellular staining for IL-17, IFN-γ, IL-4, IL-13 and Foxp3 was performed using the Foxp3 staining kit (eBiosciences). Cytokine staining was performed after re-stimulation with CD3 antibody and CD28 antibody (5 μg ml⁻¹ each) in the presence of Golgi-plug (BD Biosciences) for 5 h.

Dendritic-cell generation and isolation. Dendritic cells were expanded *in vivo* by subcutaneous injection of B16 melanoma cells secreting Flt3 ligand into the left hind flank of mice as indicated. Once tumours were visible, spleens from injected animals were dissociated in RPMI 1640 medium containing 1.67 units ml⁻¹ liberase TL (Roche) and 50 μg ml⁻¹ DNase I (Roche) for 20 min at 37 °C with shaking. EDTA was then added at a final concentration of 5 mM to stop digestion and the resulting homogenate was processed for CD11c⁺ cell isolation using the MACS mouse CD11c (N418) purification kit (Miltenyi Biotec).

***In vitro* assays.** *In vitro* Foxp3 induction assays were performed by co-culturing dendritic cells with 5.5 × 10⁴ CD4⁺CD44^{lo}CD62L^{hi}CD25⁻ naive T cells in the presence of 1 μg ml⁻¹ of CD3 antibody, 1 ng ml⁻¹ TGF-β, and 100 units ml⁻¹ IL-2, in 96-well flat-bottom plates for 4 days. For Foxp3 induction in the presence of butyrate- or TSA-pre-treated dendritic cells, TGF-β was used at 0.1 ng ml⁻¹ final concentration. *In vitro* induction assays in the absence of dendritic cells were performed by incubating 5.5 × 10⁴ naive CD4⁺ T cells with 1 ng ml⁻¹ TGF-β, 100 units ml⁻¹ IL-2, and a 1:1 cell-to-bead ratio of CD3 and CD28 T activator Dynabeads (Invitrogen). For *in vitro* suppression assays, 4 × 10⁴ naive CD4⁺ T cells were FACS-sorted from B6 mice and cultured with graded numbers of CD4⁺Foxp3⁺T_{reg} cells FACS-sorted from *Foxp3^{GFP}* mice treated with antibiotics and with or without butyrate, in the presence of 10⁵ irradiated T-cell-depleted splenocytes and 1 μg ml⁻¹ CD3 antibody in a 96-well round-bottom plate for 80 h. Proliferation of T cells was assessed by [³H]-thymidine incorporation during the final 8 h of culture.

ChIP-qPCR assays. Acetylated H3K27 ChIP-qPCR was performed as previously described²⁵. In brief, fixed cells were lysed and mono- and poly-nucleosomes were obtained by partial digestion with micrococcal nuclease (12,000 units ml⁻¹) for 1 min at 37 °C. EDTA was added to a final concentration of 50 mM to stop the reaction, and digested nuclei were resuspended in nuclear lysis buffer with 1% SDS. After sonication, 1 μg of acetylated-H3K27-specific antibody (Abcam, ab4729) was used to precipitate acetylated-H3K27-bound chromatin. Washing and de-crosslinking was performed as described previously²⁵.

Stool-sample collection. Stool samples were collected directly into sterile tubes from live mice and snap-frozen before preparation of material for SCFA quantification by HPLC or LC-MS.

HPLC assays. HPLC was carried out for analysis of derivatized stool extracts as previously described²⁴. In brief, flash-frozen stool samples were extracted with 70% ethanol and brought to a final concentration of 0.1 μg μl⁻¹. Debris was removed by centrifugation and 300 μl of supernatant was transferred to a new tube and combined with 50 μl of internal standard (2-ethylbutyric acid, 200 mM in 50% aqueous methanol), 300 μl of dehydrated pyridine 3% v/v (Wako) in ethanol, 300 μl of 250 mM *N*-(3-dimethylaminopropyl)-*N'*-ethylcarbodiimide hydrochloride (Sigma-Aldrich) in ethanol, and 300 μl of 20 mM 2-nitrophenylhydrazine hydrochloride (Tokyo Chemical) in ethanol. Samples were incubated at 60 °C for 20 min and 200 μl of potassium hydroxide 15% w/v dissolved 80/20 in methanol was added to stop the derivatization reaction. Samples were incubated again at 60 °C for 20 min and transferred into a glass conical tube containing 3 ml of 0.5 M phosphoric acid. The organic phase was extracted by shaking with 4 ml diethyl ether and transferred to a new glass conical containing water to extract any remaining aqueous compounds. The organic phase containing the derivatized SCFA was transferred into a new 5 ml glass vial and evaporated overnight in a fume hood. Derivatized SCFA were resuspended in 100 μl of mobile phase (below) and 20 μl was chromatographed on a Shimadzu HPLC system equipped with a Vydac 2.1 × 30 mm 300 A C18 column run at 200 μl per min in methanol/acetonitrile/TFA (30%/16%/0.1% v/v) and monitored for absorbance at 400 nm.

LC-MS assays. Methanol (300 μl, 80%) containing deuterated short chain fatty acid internal standards (Cambridge Isotope Laboratories) was added to 70 μl serum and incubated at -80 °C for 30 min. Samples were then centrifuged at 4 °C at 21,000g for 15 min to precipitate protein. Pure short chain fatty acid standards (Sigma-Aldrich) were also prepared in 300 μl 80% methanol containing internal standards to produce a calibration curve from 0.25 μM to 50 μM. Methanol (80%) extracts were combined with 300 μl 250 mM *N*-(3-dimethylaminopropyl)-*N'*-ethylcarbodiimide hydrochloride in ethanol, 300 μl 20 mM 2-nitrophenylhydrazine hydrochloride in ethanol and 300 μl 3% pyridine in ethanol in a glass tube and reacted at 60 °C for 20 min. The reaction was quenched with 200 μl potassium hydroxide solution (15% KOH: MeOH, 8:2 v/v) at 60 °C for 20 min. After cooling, the mixture was adjusted to pH 4 with 0.25 M HCl. Derivatized short chain fatty acids were then extracted with 4 ml ether and washed with 4 ml water before drying under a nitrogen stream. The dried sample was dissolved in 150 μl methanol, and 5 μl was injected for LC-MS analysis.

Butyrate enemas. Mice were anaesthetized with isoflurane and injected intrarectally with 200 μl of 50 mM butyric acid (pH 4) or pH-matched water delivered through a 1.2-mm-diameter polyurethane catheter (Access Technologies). Enemas were administered for 7 days.